


Synthesis of deuterium-labelled amlexanox and its metabolic stability against mouse, rat, and human microsomes

Xinmin Gan^{1,2} | Michael W. Wilson^{1,2} | Tyler S. Beyett^{3,4} | Bo Wen⁵ | Duxin Sun⁵ | Scott D. Larsen^{1,2} | John J.G. Tesmer^{6,7} | Alan R. Saltiel^{8,9} | Hollis D. Showalter^{1,2} 

¹Department of Medicinal Chemistry, University of Michigan, Ann Arbor, Michigan, USA

²Vahlteich Medicinal Chemistry Core, University of Michigan, Ann Arbor, Michigan, USA

³Program in Chemical Biology, University of Michigan, Ann Arbor, Michigan, USA

⁴Life Sciences Institute, Departments of Pharmacology and Biological Chemistry, University of Michigan, Ann Arbor, MI, United States

⁵Department of Pharmaceutical Sciences, University of Michigan, Ann Arbor, Michigan, USA

⁶Department of Biological Sciences, Purdue University, West Lafayette, Indiana, USA

⁷Department of Medicinal Chemistry and Molecular Pharmacology, Purdue University, West Lafayette, Indiana, USA

⁸Department of Medicine, Institute for Diabetes and Metabolic Health, University of California San Diego, San Diego, California, USA

⁹Department of Pharmacology, Institute for Diabetes and Metabolic Health, University of California San Diego, San Diego, California, USA

Correspondence

Hollis D. Showalter, Department of Medicinal Chemistry, University of Michigan, Ann Arbor, Michigan 48109, USA.

Email: showalh@umich.edu

Funding information

National Institutes of Health, Grant/Award Numbers: R01 DK100319 and T32-GM007767; U.S. Department of Education, Grant/Award Number: GAANN/P200A150164

As part of a program toward making analogues of amlexanox (**1**), currently under clinical investigation for the treatment of type 2 diabetes and obesity, we have synthesized derivative **5** in which deuterium has been introduced into two sites of metabolism on the C-7 isopropyl function of amlexanox. The synthesis of **5** was completed in an efficient three-step process utilizing reduction of key olefin **7b** to **8** by Wilkinson's catalyst to provide specific incorporation of di-deuterium across the double bond. Compound **5** displayed nearly equivalent potency to amlexanox (IC₅₀, 1.1 μM vs 0.6 μM, respectively) against recombinant human TBK1. When incubated with human, rat, and mouse liver microsomes, amlexanox (**1**) and *d*₂-amlexanox (**5**) were stable (*t*_{1/2} > 60 minutes) with **1** showing marginally greater stability relative to **5** except for rat liver microsomes. These data show that incorporating deuterium into two sites of metabolism does not majorly suppress Cyp-mediated metabolism relative to amlexanox.

KEYWORDS

obesity, amlexanox, *d*₂-amlexanox, metabolites, microsomal stability, TBK1 kinase, Wilkinson's catalyst

1 | INTRODUCTION

There is currently a worldwide epidemic of obesity, which is manifesting itself as a leading risk factor in industrialized countries for the development of type 2 diabetes, dyslipidemia, nonalcoholic fatty liver disease,

cardiovascular disease, and some cancers.¹ Obesity results from a sustained imbalance between caloric intake and energy expenditure and is characterized by chronic, low-grade inflammation in liver and adipose tissues, which in turn attenuates the actions of multiple hormones to produce a dysregulated metabolic state.²⁻⁴

Prior studies on the role of inflammation in the generation of insulin resistance and type 2 diabetes during obesity implicate an important role for the nuclear factor kappa-light-chain-enhancer of activated B cells (NF- κ B) pathway, revealing the role of two noncanonical inhibitors of kappa B ($\text{I}\kappa\text{B}$) kinases, TANK-binding kinase 1 (TBK1), and inhibitor of nuclear factor kappa-B kinase subunit ϵ (IKK ϵ), in insulin-independent pathways that promote energy storage and block adaptive energy expenditure during obesity.^{5,6} Since none of the currently available and widely used treatments for obesity addresses the underlying energy imbalance associated with inflammation pathways,⁷ we initiated a high throughput screen for small molecule inhibitors of the TBK1 and IKK ϵ kinases. One hit from our screen was amlexanox (**1**; Figure 1), an approved drug developed by Takeda that is used for the treatment of canker sores, asthma, and allergic rhinitis.^{8,9} The compound is a modest inhibitor of TBK1 and IKK ϵ and reproduced the effects of the IKK ϵ knockout phenotype, which include weight loss in obese mice, improved insulin sensitivity, and reduced hepatic steatosis and inflammation. Amlexanox also increased the level of the second messenger molecule cAMP and triggered the release of the hormone interleukin-6 (IL-6) from fat cells, thereby reducing the production of glucose. Two recent clinical trials indicated that amlexanox treatment effectively lowered glycated hemoglobin (HbA1c) in a subset of patients with obesity and type 2 diabetes.¹⁰ Despite these promising results, the future utility of amlexanox in the clinic for obesity and type 2 diabetes intervention may be limited by its solubility, modest potency, and/or metabolic profile.

Previous studies by Takeda investigators showed that the oral administration of amlexanox (**1**) in mice, rats, guinea pigs, and dogs generated in plasma a major mono-hydroxyl metabolite (**2**) from oxidation of the C-7 isopropyl substituent and two minor metabolites **3** and **4**^{11,12} (Figure 1). The glucuronide of **1** was also identified in rats. In humans, the main metabolite was **2**. The structures of metabolites **2** and **3** have been confirmed by synthesis.¹³

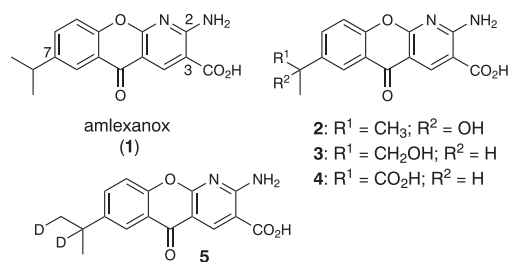


FIGURE 1 Structures of amlexanox (**1**), metabolites (**2-4**) and d_2 -amlexanox (**5**)

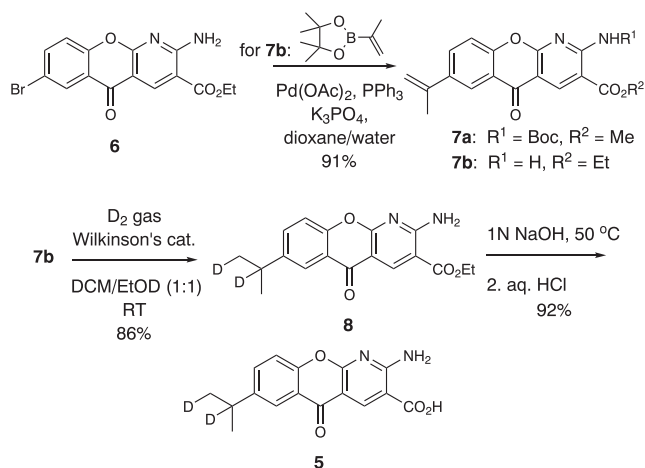
As part of a program toward making analogues of amlexanox,^{14,15} we decided to synthesize a derivative **5** (Figure 1) in which deuterium is introduced into two sites of metabolism on the C-7 isopropyl function. The deuterium kinetic isotope effect associated with placing deuterium at the site of metabolic derivatization slows metabolic activation and thus is expected to increase the lifetime of the active drug in vivo.¹⁶ Herein we provide data of the activity of **5** relative to amlexanox (**1**) in inhibiting TBK1 and its metabolic stability against mouse, rat, and human microsomes.

2 | RESULTS AND DISCUSSION

2.1 | Synthetic chemistry

Initial approaches toward generating d_1 -amlexanox, in which the benzylic C-7 methine was exchanged for deuterium, centered on catalytic exchange chemistry. Thus, reaction of amlexanox (**1**) under a variety of conditions (hydrogen gas, 10%-30% palladium on activated carbon, methanol- d_4 , 25°C-50°C) left starting material only. We then focused on incorporation of deuterium through room temperature hydrogenation of the olefin in compound **7a**, made by known procedures,^{13,17} with deuterium gas in the presence of 10% palladium on activated carbon in ethyl acetate. Thus, a control reduction of **7a** with hydrogen gave cleanly the nondeuterated C-7 isopropyl product. Substitution of deuterium for hydrogen gas yielded a new set of products with mass spectrum peaks associated with incorporation of more than two atoms of deuterium. The ¹H NMR spectrum suggested that the predominant *N*-Boc carboxylic methyl ester product had incorporated four atoms of deuterium and ¹³C NMR experiments on the next step hydrolysis product (analogous to **5**) indicated the presence of seven uniquely substituted C-7 methine carbons. This showed that deuterium had been incorporated nonspecifically into both C-7 methyl groups as well as the methine carbon. There is literature precedence for such scrambling of isotopic incorporation into benzylic and allylic sites.¹⁸

After unsuccessfully surveying other heterogeneous catalytic conditions, we then resorted to olefin reduction with a homogeneous catalyst (Scheme 1). Employing our recently published methodology of introducing C-7 substituents via late-stage coupling chemistry to make amlexanox analogues,¹⁵ we reacted tricyclic bromide **6**¹⁹ with 2-propenyl pinacol boronic ester under standard Suzuki coupling conditions to give **7b** in 91% yield. Reaction with tris(triphenylphosphine)rhodium(I) chloride (Wilkinson's catalyst) and deuterium gas,



SCHEME 1 Synthesis of d_2 -amlexanox (**5**)

as previously described for similar reductions,^{20,21} proceeded in high yield to give key intermediate **8** with specific incorporation of di-deuterium across the double bond. Standard hydrolysis conditions as described before¹⁵ then provided d_2 -amlexanox (**5**) in 92% yield and 72% overall yield from starting ester **6**. All compounds were rigorously purified by flash chromatography or crystallization, and their structural assignments are supported by diagnostic peaks in the ^1H and ^{13}C NMR spectra and by high resolution mass spectrometry. Digital copies of NMR and mass spectra can be found in Supporting Information.

The ^1H NMR spectra of the upfield region (δ 1–3 ppm) for the C-7 isopropyl substituent (Figure 2) clearly show clean, specific incorporation of di-deuterium into **5**. Complete collapse of the symmetrical pentet at δ 3.05 ppm occurs in **1** and the symmetrical doublet at δ 1.25 ppm, integrating for six protons, changes to an unsymmetrical doublet in **5** integrating for five protons. High resolution mass spectra for **5** and **8** (Supporting Information) also support specific incorporation of di-deuterium.

2.2 | Metabolic stability studies

Amlexanox (**1**) and d_2 -amlexanox (**5**) are moderately metabolized by human, rat, and mice liver microsomes. The in vitro disappearance half-life ($t_{1/2}$) of both compounds in all three microsomes is over 60 minutes (Figure 3). During the incubation in human and mice liver microsomes, about 8% more unmetabolized amlexanox remains after 60 minutes compared with d_2 -amlexanox. However, d_2 -amlexanox (**5**) is more stable than amlexanox (**1**) in rat liver microsomes. Both compounds show greater stability in human liver microsomes relative to the other microsomes. Verapamil was

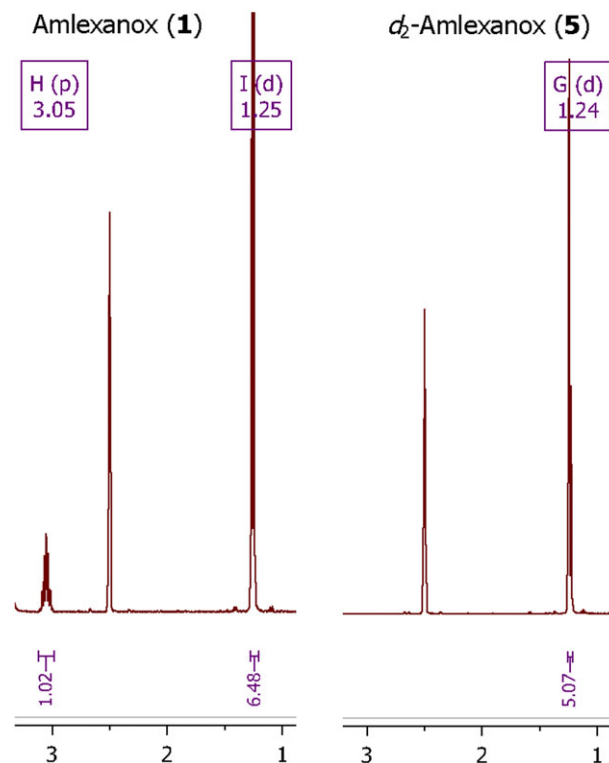


FIGURE 2 Comparison ^1H NMR spectra in $\text{DMSO-}d_6$ for C-7 substituent of amlexanox (**1**) and d_2 -amlexanox (**5**)

employed as positive control compound in order to ensure that the microsomes and NADPH used in this study were active and that incubation conditions were appropriate to perform the studies. Based on the observed degradation patterns, amlexanox (**1**) and d_2 -amlexanox (**5**) are considered to be stable against the three liver microsomes.

2.3 | Activity against TBK1 kinase

d_2 -Amlexanox (**5**) was investigated for inhibition of recombinant human TBK1 as described previously.¹⁵ The IC_{50} values shown were determined by dose-response radiometric kinase assays with myelin basic protein as substrate and are technically apparent IC_{50} values. Each is an average of three separate determinations. Since the isopropyl group on amlexanox is solvent exposed,¹⁴ incorporation of deuterium is not expected to affect inhibitor potency. Indeed, the in vitro potencies of amlexanox (**1**) and d_2 -amlexanox (**5**) against TBK1 are $0.6 \pm 0.1 \mu\text{M}$ and $1.1 \pm 0.3 \mu\text{M}$, respectively (Figure 4 and Supporting Information). The difference is not statistically significant demonstrating that amlexanox can be deuterated without affecting inhibitor potency.

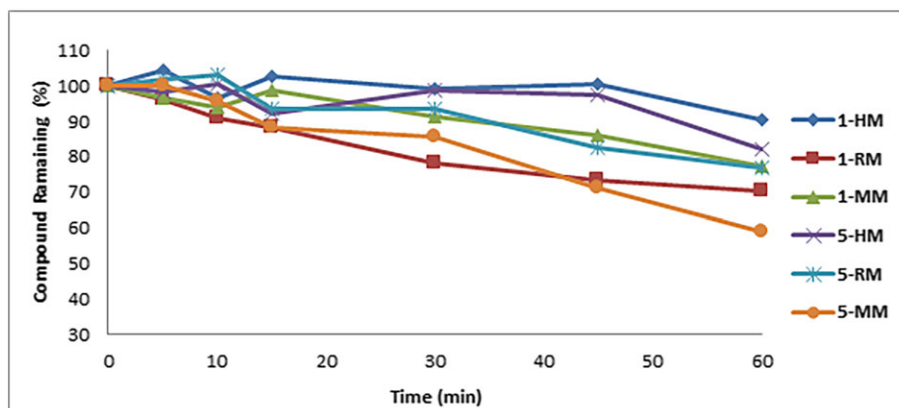


FIGURE 3 Human (H), rat (R), and mouse (M) microsomal stability for amlexanox (**1**) and d_2 -amlexanox (**5**)

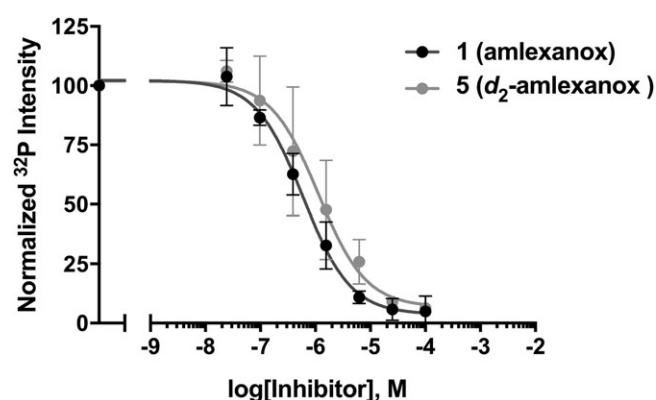


FIGURE 4 In vitro potency of amlexanox (**1**) and d_2 -amlexanox (**5**) against purified TBK1 as determined via radiometric kinase assay measuring phosphorylation of the substrate myelin basic protein. The goodness of fit (r^2) for **1** and **5** is 0.97 and 0.91, respectively, with no statistically significant difference via Student's two-tailed t test ($n = 4$, reported as mean \pm SD).

3 | CONCLUSIONS

As part of a program toward making analogues of amlexanox (**1**), which is being evaluated clinically for the treatment of type 2 diabetes and obesity, we decided to synthesize a derivative **5** to determine if placing deuterium at two sites of known metabolic activation of amlexanox might increase its half-life against three species of liver microsomes. Microsomes are rich in cytochrome (Cyp) P-450 enzymes, which are the major enzymes involved in drug metabolism and account for about 75% of total metabolism.²² The most common pathway of Cyp-mediated metabolism is hydroxylation of aliphatic carbons.

The data in Figure 3 show that amlexanox (**1**) and d_2 -amlexanox (**5**) are relatively stable against all three liver microsomes ($t_{1/2} > 60$ minutes) with amlexanox showing marginally greater stability relative to d_2 -amlexanox

except for rat liver microsomes. Hence, blocking two sites of metabolism with incorporation of a single deuterium on the C-7 methine carbon and another on a flanking methyl group of **5** does not majorly suppress Cyp-mediated metabolism relative to amlexanox. Metabolite identification experiments will be required to expand upon these findings. Additionally, synthetic chemistry needs to be developed that can specifically incorporate C-7 deuterium patterns (eg, $-\text{CH}(\text{CH}_3)(\text{CH}_2\text{D})$ and $-\text{CD}(\text{CH}_3)_2$) aligned with known metabolites **2-4** and additional patterns (eg, $-\text{CH}(\text{CD}_3)_2$, $-\text{CD}(\text{CD}_3)_2$) to more fully explore the deuterium isotope effect.

4 | EXPERIMENTAL

4.1 | Materials and instrumentation

All starting monomers were obtained from commercial suppliers and were used without further purification. Routine ^1H NMR spectra were recorded at 400 or 500 MHz on a Varian 400 or 500 instrument, respectively, with CDCl_3 or $\text{DMSO}-d_6$ as solvent. Chemical shift values are recorded in δ units (ppm). High resolution mass spectrometry (HRMS) analysis was performed on an Agilent Q-TOF system. Analytical HPLC was performed on an Agilent 1100 series instrument with an Agilent Zorbax Eclipse Plus C18 (4.6 mm \times 75 mm, 3.5- μm particle size) column with the gradient 10% acetonitrile/water (1 min), 10% to 90% acetonitrile/water (6 minutes), and 90% acetonitrile/water (2 minutes) flow = 1 mL/minute. Thin-layer chromatography (TLC) was performed on silica gel GHLF plates (250 μm) purchased from Analtech. Column chromatography was carried out in the flash mode utilizing silica gel (220-240 mesh) purchased from Silicycle. Extraction solutions were dried over anhydrous sodium sulfate prior to concentration.

4.2 | Ethyl 2-amino-5-oxo-7-(prop-1-en-2-yl)-5H-chromeno[2,3-b]pyridine-3-carboxylate (7b)

A solution of tripotassium phosphate (2.63 g, 12.4 mmol) in water (6 mL) was added to a nitrogen-degassed suspension of ethyl 2-amino-7-bromo-5-oxo-5H-chromeno[2,3-b]pyridine-3-carboxylate¹⁹ (**6**; 750 mg, 2.07 mmol), 4,4,5,5-tetramethyl-2-(prop-1-en-2-yl)-1,3,2-dioxaborolane (833 mg, 4.96 mmol), triphenylphosphine (271 mg, 1.03 mmol), and Pd(OAc)₂ (60.3 mg, 0.27 mmol) in *p*-dioxane (60 mL) in a 500- mL RB flask. The mixture was heated at 100°C to 105°C under nitrogen for 2 hours. After cooling, the mixture was diluted with water (50 mL) and extracted with dichloromethane (2 × 120 mL). The combined organic phases were dried (Na₂SO₄) and concentrated to leave an orange solid that was triturated sequentially with small volumes of ethanol and ethyl ether, collected, and dried to leave **7b** (610 mg, 91%) as a white solid: mp 245°C to 247°C. ¹H NMR (400 MHz, chloroform-*d*): δ 9.16 (s, 1H), 8.38 (s, 1H), 8.31 (d, *J* = 2.3 Hz, 1H), 7.86 (dd, *J* = 8.8, 2.4 Hz, 1H), 7.47 (d, *J* = 8.7 Hz, 1H), 5.86 (s, 1H), 5.49 (d, *J* = 1.3 Hz, 1H), 5.23-5.18 (m, 1H), 4.41 (q, *J* = 7.1 Hz, 2H), 2.24 (dd, *J* = 1.5, 0.8 Hz, 3H), 1.45 (t, *J* = 7.1 Hz, 3H). HRMS: *m/z* (M + H)⁺ Calcd. for C₁₈H₁₆N₂O₄: 325.1183; Found 325.1188.

4.3 | Ethyl 2-amino-5-oxo-7-(propan-2-yl-1,2-*d*₂)-5H-chromeno[2,3-b]pyridine-3-carboxylate (8)

Tris(triphenylphosphine)rhodium(I) chloride (Wilkinson's catalyst; 339 mg, 0.366 mmol) was completely dissolved in anhydrous dichloromethane (10 mL) and ethanol-*d*₁ (10 mL) in a 250- mL three-neck RB flask under nitrogen. The flask with the resulting clear red brown solution was evacuated by a water pump and then flushed with deuterium gas in a balloon. This flushing/evacuation procedure was repeated three more times, and then the mixture was stirred under deuterium gas (balloon pressure) for 20 minutes at room temperature. Then compound **7** (360 mg, 1.11 mmol) dissolved in a mixture of warm dichloromethane (75 mL) and ethanol-*d*₁ (75 mL) was added by syringe. The resulting solution was stirred at room temperature for 4.5 hours and then concentrated to a solid that was triturated in a small volume of benzene. The collected solids were further purified by flash silica gel column chromatography (elution with 0.5%-1.0% methanol in dichloromethane). Product fractions were combined and concentrated to leave **8** (315 mg, 86%) as a white solid: mp 239°C to 241°C. ¹H NMR (400 MHz, chloroform-*d*): δ 9.16

(s, 1H), 8.34 (s, 1H), 8.11 (d, *J* = 2.3 Hz, 1H), 7.59 (dd, *J* = 8.6, 2.3 Hz, 1H), 7.44 (d, *J* = 8.6 Hz, 1H), 5.84 (s, 1H), 4.41 (q, *J* = 7.1 Hz, 2H), 1.44 (t, *J* = 7.1 Hz, 3H), 1.30 (d, *J* = 6.5 Hz, 5H). HRMS: *m/z* (M + H)⁺ Calcd. for C₁₈H₁₆D₂N₂O₄: 329.1465; Found 329.1480.

4.4 | 2-Amino-5-oxo-7-(propan-2-yl-1,2-*d*₂)-5H-chromeno[2,3-b]pyridine-3-carboxylic acid (*d*₂-amlexanox; **5**)

To a suspension of **8** (460 mg, 1.4 mmol) in ethanol (80 mL) and water (10 mL) was added 1 N aq. NaOH (10 mL), and the mixture was stirred at 50°C for 90 minutes. TLC (5% methanol in dichloromethane) showed consumption of starting material. The mixture was filtered, and the filtrate concentrated to a wet solid that dissolved in water (50 mL). The solution was acidified with 1 N aq. HCl to pH ~3, and the precipitated solids were stirred at room temperature for 20 hours. After storage at room temperature for another 24 hours, the solids were collected, washed with water, and dried under vacuum at 60°C for 4 hours to leave **5** (385 mg, 92%) as an off-white solid: mp > 300°C (dec.). ¹H NMR (500 MHz, DMSO-*d*₆): δ 13.45 (s, 1H), 8.80 (s, 1H), 8.25 (b, 2H), 7.92 (d, *J* = 2.3 Hz, 1H), 7.73 (dd, *J* = 8.6, 2.4 Hz, 1H), 7.53 (d, *J* = 8.6 Hz, 1H), 1.24 (d, *J* = 8.6 Hz, 5H). ¹³C NMR (101 MHz, DMSO-*d*₆): δ 174.84, 167.35, 162.25, 161.46, 153.02, 144.93, 141.35, 133.71, 122.44, 120.91, 118.04, 106.23, 105.94, 33.70 – 31.07 (m), 23.64, 23.58 – 23.11 (m). HRMS: *m/z* (M + H)⁺ Calcd. for C₁₆H₁₂D₂N₂O₄: 301.1152; Found 301.1157. HPLC: *t*_R, 6.42, purity 98.3%.

4.5 | Metabolic stability studies

The in vitro metabolism study of amlexanox and *d*₂-amlexanox were performed in human, rat, and mice liver microsomes to evaluate the potential of each compound for cytochrome P450-mediated metabolism. The metabolic stability was assessed as described using pooled CD-1 mouse liver microsomes, pooled SD rat liver microsomes, and pooled human liver microsomes (purchased from Xeno Tech); 1 μM of each compound was incubated with 0.5-mg/mL liver microsomes and 1.7 mM cofactor β-NADPH in 0.1 M phosphate buffer (pH = 7.4) containing 3.3 mM MgCl₂ at 37°C. The DMSO concentration was less than 0.1% in the final incubation mixture. At 0, 5, 10, 15, 30, 45, and 60 minutes of incubation, 40 μL of reaction mixture were removed, and the reaction stopped immediately by adding three-fold excess of cold acetonitrile containing 100 ng/mL of internal standard for quantification. The incubation without the

addition of NADPH was used as a negative control. Verapamil was incubated similarly as a positive control substrate. The collected fractions were centrifuged at 15 000 rpm for 10 minutes to collect the supernatant for LC-MS/MS analysis, from which the amount of remaining compound was determined. The natural log of the amount of compound remaining was plotted against time to determine the disappearance rate and the half-life of tested compounds. The LC-MS/MS method consisted of a Shimadzu HPLC system and chromatographic separation of tested compound was achieved using a Waters XBridge-C18 column (5 cm × 4.6 mm, 3.5 μm). An AB Sciex QTrap 5500 mass spectrometer equipped with an electrospray ionization source (Applied Biosystems, Toronto, Canada) in the negative-ion multiple reaction monitoring (MRM) mode for detection. The mobile phases were 0.1% formic acid in purified water (A) and 0.1% formic acid in acetonitrile (B). The gradient (B) was held at 10% (0–0.5 minute), increased to 95% at 2 minutes, kept at isocratic 95% B for 1.0 minute, and then immediately stepped back down to 10% for a 2-minute re-equilibration. Flow rate was set at 1.0 mL/minute. Amlexanox, *d*₂-amlexanox, and internal standard 4-ASA were detected on the mass spectrometer by using multiple reaction monitoring transitions 297.1 → 253.2 *m/z*, 299.2 → 255.1 *m/z*, and 152.0 → 108.0 *m/z*, respectively. Mass spectrometry parameter optimization was performed using an automated quantitative method provided by the manufacturer.

4.6 | Kinase assay

The assay was performed as described previously.¹⁵ Briefly, 50nM purified TBK1 was incubated with 5μM myelin basic protein and varying concentrations of inhibitor (from 10μM to 0μM). Reactions were initiated by the addition of 10μM ATP spiked with [γ -³²P]-ATP and allowed to proceed for 30 minutes at room temperature. After quenching the reactions, radioactive phosphorylated substrate was quantified via phosphorimaging plates. Results were analyzed with GraphPad Prism 7 and fit to an inhibition dose-response sigmoidal curve with the Hill slope constrained to −1. Assays were repeated four independent times, and the results reported as mean ± standard deviation. Statistical significance was determined via Student's two-tailed *t* test (*P* < 0.05).

ACKNOWLEDGMENTS

This study was supported by National Institutes of Health (NIH) Pharmacological Sciences Training Program fellowship (T32-GM007767) and US Department of

Education GAANN fellowship (P200A150164) to T.S.B. and NIH R01 DK100319 to X.G., J.J.G.T., A.R.S., and H.D.S.

CONFLICT OF INTEREST

The authors report no conflicts of interest.

ORCID

Hollis D. Showalter  <https://orcid.org/0000-0003-2863-0170>

REFERENCES

1. Giordano A, Frontini A, Cinti S. Convertible visceral fat as a therapeutic target to curb obesity. *Nat Rev Drug Discov*. 2016; 15(6):405–424.
2. Saltiel AR. New therapeutic approaches for the treatment of obesity. *Sci Transl Med*. 2016;8(323 323rv2):1–11.
3. Mowers J, Uhm M, Reilly SM, et al. Inflammation produces catecholamine resistance in obesity via activation of PDE3B by the protein kinases IKKε and TBK1. *Elife*. 2013;2:e01119 /01111-01118. <https://doi.org/10.7554/elife.01119>
4. Reilly SM, Saltiel AR. Adapting to obesity with adipose tissue inflammation. *Nat Rev Endocrinol*. 2017;13(11):633–643.
5. Chiang S-H, Bazuine M, Lumeng CN, et al. The protein kinase IKKε regulates energy balance in obese mice. *Cell (Cambridge, MA, U S)*. 2009;138(5):961–975.
6. Saltiel AR. Insulin resistance in the defense against obesity. *Cell Metab*. 2012;15(6):798–804.
7. Clapham JC, Arch JRS. Targeting thermogenesis and related pathways in anti-obesity drug discovery. *Pharmacol Ther*. 2011; 131(3):295–308.
8. Makino H, Saijo T, Ashida Y, Kuriki H, Maki Y. Mechanism of action of an antiallergic agent, amlexanox (AA-673), in inhibiting histamine release from mast cells. Acceleration of cAMP generation and inhibition of phosphodiesterase. *Int Arch Allergy Appl Immunol*. 1987;82(1):66–71.
9. Bell J. Amlexanox for the treatment of recurrent aphthous ulcers. *Clin Drug Investig*. 2005;25(9):555–566.
10. Oral EA, Reilly SM, Gomez AV, et al. Inhibition of IKKε and TBK1 improves glucose control in a subset of patients with type 2 diabetes. *Cell Metab*. 2017;26(1):157–170. e157
11. Torii H, Yoshida K, Tsukamoto T, et al. Metabolic fate of amoxanox (AA-673), a new antiallergic agent, in rats, mice, guinea pigs and dogs. *Yakuri to Chiryō*. 1985;13(9):4933–4954.
12. Yoshida K, Danayama K. Pharmacokinetics and metabolism of amlexanox (AA-673), a new antiallergic agent, after nasal administration to rats. *Yakuri to Chiryō*. 1987;15(5):1873–1881.
13. Ukawa K, Ishiguro T, Kuriki H, Nohara A. Synthesis of the metabolites and degradation products of 2-amino-7-isopropyl-5-oxo-5H-[1]benzopyrano[2,3-*b*]pyridine-3-carboxylic acid (amoxanox). *Chem Pharm Bull*. 1985;33(10):4432–4437.
14. Beyett TS, Gan X, Reilly SM, et al. Carboxylic acid derivatives of amlexanox display enhanced potency toward TBK1 and IKKε

- and reveal mechanisms for selective inhibition. *Mol Pharmacol*. 2018;94(4):1210-1219.
15. Beyett TS, Gan X, Reilly SM, et al. Design, synthesis, and biological activity of substituted 2-amino-5-oxo-5H-chromeno[2,3-b]pyridine-3-carboxylic acid derivatives as inhibitors of the inflammatory kinases TBK1 and IKK ϵ for the treatment of obesity. *Bioorg Med Chem*. 2018;26(20):5443-5461.
 16. Shao L, Hewitt MC. The kinetic isotope effect in the search for deuterated drugs. *Drug News Perspect*. 2010;23(6):398-404.
 17. Saltiel AR, Showalter HD, Larsen S. Preparation of deuterated amlexanox derivatives for use as TBK1 or IKK ϵ protein kinase inhibitors. US Patent 9,944,652, Apr. 17, 2018.
 18. Nishimura S. *Handbook of Heterogeneous Catalytic Hydrogenation for Organic Synthesis*. New York: John Wiley & Sons; 2001. Chapter 3:68-72.
 19. Ghosh C, Sinharoy DK, Mukhopadhyay KK. Heterocyclic systems. Part 6. Reactions of 4-oxo-4H-[1]benzopyran-3-carbonitriles with hydrazine, phenylhydrazine, hydroxylamine, and some reactive methylene compounds. *J Chem Soc, Perkin Trans 1*. 1979;8:1964-1968.
 20. Rakoff H. Preparation of fatty acids and esters containing deuterium. *Prog Lipid Res*. 1982;21(3):225-254.
 21. Lie Ken Jie MSF, Choi YC. Mass spectral studies of deuterium-labeled picolinyl fatty esters in the determination of double-bond positions. *J Am Oil Chem Soc*. 1992;69(12):1245-1247.
 22. Guengerich FP. Cytochrome P450 and chemical toxicology. *Chem Res Toxicol*. 2008;21(1):70-83.

SUPPORTING INFORMATION

Additional supporting information may be found online in the Supporting Information section at the end of the article.

How to cite this article: Gan X, Wilson MW, Beyett TS, et al. Synthesis of deuterium-labelled amlexanox and its metabolic stability against mouse, rat, and human microsomes. *J Label Compd Radiopharm*. 2019;62:202-208. <https://doi.org/10.1002/jlcr.3716>